Time-Dependent Relaxation of Strained Silicon-on-Insulator Lines Using a Partially Coherent X-Ray Nanobeam

F. Mastropietro,[1,2,*] J. Eymery,[1] G. Carbone,[2] S. Baudot,[1,3] F. Andrieu,[3] and V. Favre-Nicolin[1,4,5,†]

[1]*CEA-UJF, INAC, SP2M, 38054 Grenoble, France*
[2]*European Synchrotron Radiation Facility, F-38043 Grenoble, France*
[3]*CEA-LETI, Minatec, 38054 Grenoble, France*
[4]*Université Grenoble-Alpes, F-38041 Grenoble, France*
[5]*Institut Universitaire de France, F-75005 Paris, France*

(Received 17 June 2013; revised manuscript received 23 September 2013; published 19 November 2013)

We report on the quantitative determination of the strain map in a strained silicon-on-insulator line with a 200×70 nm^2 cross section. In order to study a single line as a function of time, we used an x-ray nanobeam with relaxed coherence properties as a compromise between beam size, coherence, and intensity. We demonstrate how it is possible to refine the line deformation map at the nanoscale, and follow its evolution as the line relaxes under the influence of the x-ray nanobeam. We find that the strained line flattens itself under irradiation but maintains the same linear strain (ϵ_{zz} unchanged).

DOI: 10.1103/PhysRevLett.111.215502 PACS numbers: 61.05.C−, 68.60.Bs, 41.50.+h

New applications in optoelectronic and electronic semiconductor devices have been achieved by a careful control of strain at the nanoscale level. Several physical properties such as charge carrier mobility in transistors and emission wavelength in quantum dots or well heterostructure have been advantageously improved by applying strain fields adapted to the materials' band structure, orientation, and doping features [1–4].

The measurement of these strain fields has required the development of dedicated techniques with adapted spatial and strain resolution. Electronic imaging techniques have seen tremendous developments and outstanding achievements [5], but are always limited by the preparation of thin foil that can considerably relieve internal stress in nanostructures. Very recently, x-ray diffraction has taken profit of the highly brilliant and coherent radiation provided by synchrotron sources [6]. Moreover, the optimization of dedicated focusing optics (compound refractive lenses [7], Fresnel zone plate (FZP) [8,9], Kirkpatrick-Baez mirrors [10,11]) has allowed the use of nanobeams, increasing the spatial resolution of diffraction measurements. This also allowed the use of coherent x-ray diffraction imaging for structure (shape, size) and strain determination of single nano-objects [12–16].

In this Letter, we illustrate how the strain of a single strained silicon nanostructure changes during irradiation with x rays, as a function of measurement time using a partially coherent x-ray nanobeam. Strained silicon-on-insulator (SSOI) lines are considered due to their strong interest in enhancing the carrier mobility in metal oxide semiconductors field-effect-transistor (MOSFET) devices [17,18].

Silicon lines were etched from a (001) oriented SSOI substrate made by a wafer bonding technique from the Si deposition on a SiGe virtual substrate imposing a biaxial strain, as described in [19]. Lines in tensile strain ($\epsilon_{yy} = +0.78\%$) are oriented along the $[1\bar{1}0]$ direction which corresponds to the usual direction of *n*-MOSFET channels for which electron transport is improved. The strain relaxes elastically along [110], i.e., perpendicularly to the lines [18]. An in-plane misorientation of about 1° is used between the strained Si lines and the Si substrate in order to separate the line and substrate Bragg peaks. The SSOI lines have a width $W = 225$ nm and a height $H = 70$ nm (Fig. 1) and lie on a 145 nm SiO_2 layer. The distance d between two adjacent lines is about 775 nm. Grazing-incidence x-ray diffraction have been performed on these line gratings [18] and gave $\epsilon_{xx} = +0.04\%$ (almost fully relaxed along the line direction [110]) and $\epsilon_{yy} = +0.74\%$, which is very close to the biaxial strain before etching. Linear elasticity calculations allow estimating $\epsilon_{zz} \approx -0.25(5)\%$ from elastic constants.

As recently proven, the displacement field of this system can be probed using coherent beams [15]. However, in the present system the SSOI line period is about one micron, so that a *single* line can only be studied using a highly focused x-ray beam. The experiment has been conducted on the undulator beam line id01 of the European Synchrotron Radiation Facility, using a 8 keV energy beam obtained with a Si(111) channel cut monochromator. The x-ray beam has been focused to the sample position using a gold FZP with a diameter of 200 μm and a 70 nm outermost zone width [8]. A beam stop and a pinhole have been used to cut the contribution of the central part of the direct beam and the higher diffraction orders.

The asymmetric $(1\bar{1}3)$ Bragg reflection has been probed during the experiment to reduce the contribution of the Si substrate. In addition, in the considered geometry, the detection plane is almost tangent to Ewald's sphere and thus the information about the displacement fields is

 © 2013 American Physical Society

contained in a single image. The incoming radiation is inclined with respect to the sample surface by $\alpha_i = 52.3°$ and the diffracted beam is collected with a Maxipix detector [20] at $2\theta_f = 56.48°$.

In this experiment the transverse coherence length is estimated to $11(h) \times 53(v)\ \mu\text{m}^2$ at the location of the FZP (49 m from the source), due to the combined effects of the undulator source size and the monochromator [21]. Thus, to achieve a highly coherent x-ray beam, a partial illumination of the FZP can be used [22]. However, this would lead to a significant increase in the horizontal size of the focused beam (horizontal FWHM of the order of 1 μm). In order to illuminate a *single* SSOI line, it is therefore necessary to use a partially coherent x-ray beam by using the entire FZP rather than a small area corresponding to the transverse coherence length.

The use of partially coherent x-ray beams has recently been at the focus of a number of studies, [23,24] and it was also demonstrated that quantitative reconstructions using *ab initio* phase retrieval algorithms were possible in such a case [25,26]. The present study differs from these previous ones: first, the x-ray beam illuminating the FZP is more than 10 times larger than the transverse coherence length in the horizontal direction, thus introducing a significant blur in the diffraction image. Second, the size of the focal point ideally produced by a point source placed at 49 m from the FZP is much smaller than the width of the SSOI line. This is illustrated in Fig. 1, where the cross section of the SSOI line is compared to the shapes of ideal and partially coherent beams, and in Fig. 2, showing the blurring effect on the diffraction of reflection $(1\bar{1}3)$. As the size of the source increases the focal point by a factor ≈ 3, the

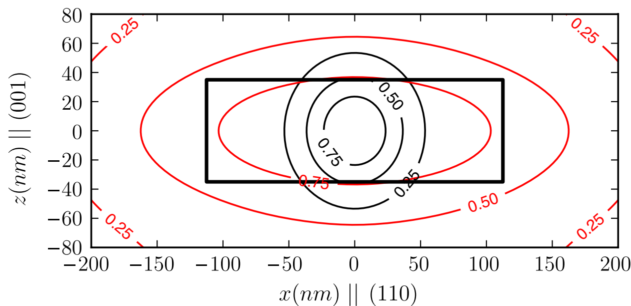

FIG. 1 (color online). Nanofocused x-ray beam at the sample position: (heavy black line) sketch of the rectangular cross section of the SSOI line, $225 \times 70\ \text{nm}^2$; (black contour levels) normalized intensity distribution at the sample position, calculated using a point source 49 m from the fully illuminated Fresnel zone plate; (red contour levels) normalized intensity distribution taking into account the source size ($64 \times 13.8\ \mu\text{m}^2$ r.m.s.) for the id01 beam line. Contour levels are represented at 25%, 50%, and 75% of the maximum intensity. The calculations are made at 150 μm from the focal point, i.e., the estimated position for the sample. The resulting illumination of the SSOI line is both partially coherent and inhomogeneous.

simultaneous reconstruction of the object and the coherence function—as proposed in [27]—becomes difficult.

In order to make a quantitative analysis of the recorded diffraction images, we used a direct approach to calculate the effect of partial coherence and inhomogeneous illumination (each part of the source being focused on different parts of the SOI line) from the characteristics of the undulator source: (i) the undulator source was modeled as a superposition of incoherent point sources [28], with a Gaussian intensity distribution [$64(h) \times 13.8(v)\ \mu\text{m}^2$ r.m.s. source size]. To limit the computational requirements, a rectangular array of 9×5 sources was taken into account. Then, (ii) the complex amplitude, focused by the FZP, was calculated at the sample position (at each atomic position in a 2D layer of the silicon line), for each of the 45 point sources. Finally, (iii) the intensity on the detector was calculated as the incoherent sum of the intensities contributed by all the point sources. The FZP was modeled as a grating with an ideal series of concentric rings of radius $r_n = \sqrt{n\lambda f}$, where n is the order of the ring, λ the wavelength, and f the focal length.

A time-dependent study has been performed illuminating for 3000 s the same section of the selected line with the aim of inducing radiation damage at the Si/SiO_2 interface, and investigate its nature and its characteristic time. In our experimental conditions, the x-ray beam carries in term of photon flux $\approx 5 \times 10^4$ photons/(s nm^2). Several 2D diffraction patterns of the described Bragg peak have been collected during the experiment with an acquisition time of 100 s. The most relevant detector images are shown in Figs. 3(a), 3(c), 3(e), and 3(g) corresponding to the times $T = 0$, 800, 1600, 2900 s. The oscillations along L are directly related to the thickness (≈ 70 nm) of the SOI line. The "banana-shaped" intensity distribution observed in the [110] direction is a consequence of the spontaneous bending induced by the free-surface strain relaxation already observed [30]. This strain is relaxed during the x-ray exposure.

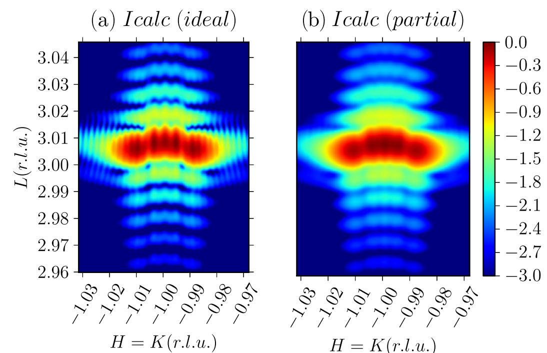

FIG. 2 (color online). Diffraction from a SSOI line by a partially coherent x-ray nanobeam [$(1\bar{1}3)$ reflection], calculated from a simulated deformation of the SSOI line, using either (a) a plane wave illumination or (b) taking into account the partially coherent illumination of the FZP.

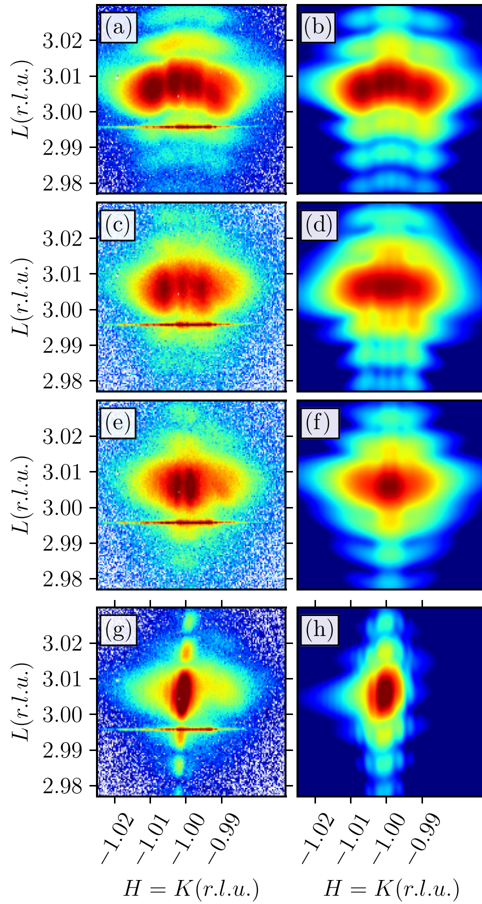

FIG. 3 (color online). (a), (c), (e), (g) Two-dimensional diffraction patterns compared to (b), (d), (f), (h) calculations for the chosen silicon line at different times $T = 0$, 800, 1600, and 2900 s. Relevant changes are visible in the experimental intensity distribution and well reproduced by calculations. Intensities are expressed using the same logarithmic color scale, with a total amplitude spanning 3 orders of magnitude. The horizontal stripe near $l = 2.996$ is due to the Si substrate, and was masked during the refinement. The slight bending visible in (g) is due to a small ($< 0.1°$) rotation of the line [see Fig. 4(d)] around the irradiation, which results in a twisting along the $[1\bar{1}0]$ direction, and cannot be reproduced in a 2D model.

In order to determine the deformation field inside the SOI line as a function of time, it was not possible to use standard imaging algorithms based on *ab initio* phase retrieval, due to the high degree of partial coherence. Since the SOI lines are perfectly crystalline, we have therefore opted to perform a direct refinement of the 2D displacement field in the plane perpendicular to the direction of the SOI line. The line was modeled as a perfect silicon crystal, with a 70×225 nm^2 cross section, and the displacement of the atoms was described using a polynomial sum: $u_z(x, z) = \sum a_{n_x,n_z} x^{n_x} z^{n_z}$, with $0 <= n_x <= 4$ and $0 <= n_z <= 2$.

This model allows the description of asymmetric displacements inside the SOI line, and is generic enough to

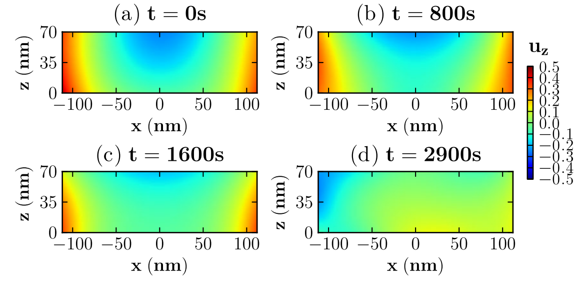

FIG. 4 (color online). Displacement fields u_z obtained from the time-dependent analysis of radiation damage at $T = 0$, 800, 1600, and 2900 s. The u_z profiles is visibly less curved at $T = 2900$ s (d) with respect to the one obtained at (a) $T = 0$. Scale units expressed in nanometers are represented by colors.

allow us to describe any realistic continuous displacement field. Diffraction near the $(1\bar{1}3)$ reflection is not sensitive to displacement in the horizontal (x in Fig. 1) [110] direction (perpendicular to the scattering vector) and the displacement field along the direction of the line (y) is assumed to be negligible due to mechanical constraints along this direction.

The scattering is calculated by generating the position of all Si atoms in the xz plane from the u_z displacement field, and uses the PyNX library [31], which allows fast computing using a graphical processing unit. This method also avoids approximating the scattering as the Fourier transform of $\rho(\vec{r})\exp[2i\pi\vec{s}\cdot\overrightarrow{\mathrm{u(r)}}]$ (where ρ and $\vec{u}$ are the average electronic density and displacement at position $\vec{r}$ in the crystal), which is frequently used for Bragg coherent x-ray scattering but can be incorrect in the presence of a large inhomogeneous displacement field [32].

The u_z polynomial is minimized using first a parallel simulated annealing algorithm [33], with 50 000 trials, followed by a least-squares minimization. The criterion for minimization is $\chi^2 = \sum_i \omega_i (I^i_{\mathrm{obs}} - \alpha I^i_{\mathrm{calc}})^2$, where α is a scale factor, and the weight ω_i is equal to $1/I^i_{\mathrm{obs}}$ if $I^i_{\mathrm{obs}} > 0$, and 0 otherwise.

The resulting calculated scattering patterns obtained by fitting the experimental data are shown in Fig. 3. The corresponding displacement fields are depicted in Fig. 4. u_z visibly changes from $T = 0$ (a) to $T = 2900$ s (d), where it shows a quite less curved profile. The strain fields ϵ_{zx} and ϵ_{zz} can be easily calculated from u_z: the standard deviations of ϵ_{zx} and the mean values of ϵ_{zz} are summarized in Table I. $\langle\sqrt{\langle\epsilon^2_{zx}\rangle}\rangle$ decreases continuously during

TABLE I. Mean strain values at $T = 0$, 800, 1600, and 2900 s.

Strain	0 s	800 s	1600 s	2900 s
$\sqrt{\langle\epsilon^2_{zx}\rangle}$	0.63%	0.57%	0.45%	0.19%
$\langle\epsilon_{zz}\rangle$	−0.19%	−0.21%	−0.21%	−0.18%

the relaxation process while $\langle \epsilon_{zz} \rangle$ remains around the same value.

Radiation damage resulting from the highly brilliant beam has been observed both for macromolecular compounds [34] and semiconductor structure [35,36]. A bending of unstrained SOI lines was previously reported and attributed to the underlying oxide structural expansion [37]. In this article we show how it is possible to follow quantitatively the evolution of the 2d strain field.

In the present system, the SOI line remains crystalline during the long x-ray exposure, as demonstrated by the continued presence of a Bragg diffraction spot. Moreover, we have shown that the shape of the diffraction peak can be explained by a simple elastic deformation of the line. The relaxation of the line is due to radiation damage occurring at the interface between the silicon line and the underlying SiO_2 [35]. There is no significant change with time of the period of the fringes corresponding to the 70 nm thickness, indicating that any damage at the interface does not extend significantly into the silicon line.

It should be noted that $\langle \epsilon_{zz} \rangle$ does not vary despite the clear relaxation: this difference in the evolution between ϵ_{zz} and ϵ_{xz} is due to the fact that only the part of the SOI line around the incident beam is relaxed, and therefore the line remains stressed (in tension) where the Si/SiO_2 interface is not damaged. This is a very important result for MOSFET, as a significant alteration to the Si/SiO_2 interface would not affect conduction properties. Finally, the shape of the diffraction spot remains unchanged after waiting 10 min without illumination from an x-ray beam, indicating that direct heating effects (dilatation) are negligible. This indicates that while the irradiation changes the strain state of the line, it affects mostly its curvature, and has little effect of the linear strain value and therefore on the enhanced mobility (see [1,38] for a discussion on the strain reliability in MOSFET devices).

To conclude, we have shown that it is possible to retrieve the strain field inside a single SOI line, and follow its evolution as a function of time during irradiation with an intense x-ray beam. This information can be retrieved even though we used a partially coherent beam in order to optimize both the flux and the beam size on the sample. The refinement method which is used here to take into account partial coherence can be applied to any synchrotron beam line using a submicron beam, as long as the source and focusing optics are correctly modeled. Moreover, the use of a strongly asymmetric reflection allowed the data collection of a scattering plane containing all the relevant information about the two-dimensional relaxation of the line, using single two-dimensional frames.

The intense irradiation only damaged the Si/SiO_2 interface and not the crystalline silicon structure, which furthermore keeps the strong normal strain essential to the conduction properties. This demonstration paves the way for the study of complex, working devices such as MOSFET: this has already been conducted on micron-sized FET, [39] but the *in situ* analysis of FET on industrially relevant devices will require very small and intense probes, i.e., x-ray beams exploiting the full intensity of undulator source while avoiding strict coherence constraints.

This work was partially supported by the French ANR XDISPE (ANR-11-JS10-004-01). The authors would like to thank the id01 staff for help during the experiment, and the European Synchrotron Radiation Facility for providing the beamtime.

*Present address: IM2NP, Université Aix-Marseille, France.

†Vincent.Favre-Nicolin@cea.fr

[1] M. L. Lee, E. A. Fitzgerald, M. T. Bulsara, M. T. Currie, and A. Lochtefeld, J. Appl. Phys. **97**, 011101 (2005).
[2] P. Bhattacharya, S. Ghosh, and A. Stiff-Roberts, Annu. Rev. Mater. Res. **34**, 1 (2004).
[3] C. E. Pryor and M.-E. Pistol, Phys. Rev. B **72**, 205311 (2005).
[4] R. S. Jacobsen *et al.*, Nature (London) **441**, 199 (2006).
[5] F. Hüe, M. Hÿtch, H. Bender, F. Houdellier, and A. Claverie, Phys. Rev. Lett. **100**, 156602 (2008).
[6] K. A. Nugent, Adv. Phys. **59**, 1 (2010).
[7] A. Snigirev, V. Kohn, I. Snigireva, A. Souvorov, and B. Lengeler, Appl. Opt. **37**, 653 (1998).
[8] K. Jefimovs, O. Bunk, F. Pfeiffer, D. Grolimund, J. van der Veen, and C. David, Microelectron. Eng. **84**, 1467 (2007).
[9] S. Gorelick, J. Vila-Comamala, V. A. Guzenko, R. Barrett, M. Salomé, and C. David, J. Synchrotron Radiat. **18**, 442 (2011).
[10] P. Kirkpatrick and A. V. Baez, J. Opt. Soc. Am. **38**, 766 (1948).
[11] D. Paganin, *Coherent X-Ray Optics* (Oxford University, New York, 2006).
[12] C. G. Schroer, P. Boye, J. M. Feldkamp, J. Patommel, A. Schropp, A. Schwab, S. Stephan, M. Burghammer, S. Schoder, and C. Riekel, Phys. Rev. Lett. **101**, 090801 (2008).
[13] I. Robinson and R. Harder, Nat. Mater. **8**, 291 (2009).
[14] M. C. Newton, S. J. Leake, R. Harder, and I. K. Robinson, Nat. Mater. **9**, 120 (2010).
[15] M. C. Newton, R. Harder, X. Huang, G. Xiong, and I. K. Robinson, Phys. Rev. B **82**, 165436 (2010).
[16] V. L. R. Jacques, S. Ravy, D. Le Bolloc'h, E. Pinsolle, M. Sauvage-Simkin, and F. Livet, Phys. Rev. Lett. **106**, 065502 (2011).
[17] F. Andrieu *et al.*, in *2007 IEEE Symposium on VLSI Technology* (IEEE, Kyoto, 2007), p. 50.
[18] S. Baudot, F. Andrieu, F. Rieutord, and J. Eymery, J. Appl. Phys. **105**, 114302 (2009).
[19] B. Ghyselen *et al.*, Solid State Electron. **48**, 1285 (2004).
[20] C. Ponchut, J. M. Rigal, J. Clément, E. Papillon, A. Homs, and S. Petitdemange, JINST **6**, C01069 (2011).
[21] A. Diaz, C. Mocuta, J. Stangl, M. Keplinger, T. Weitkamp, F. Pfeiffer, C. David, T. H. Metzger, and G. Bauer, J. Synchrotron Radiat. **17**, 299 (2010).

[22] F. Mastropietro, D. Carbone, A. Diaz, J. Eymery, A. Sentenac, T. H. Metzger, V. Chamard, and V. Favre-Nicolin, Opt. Express **19**, 19 223 (2011).
[23] S. Flewett, H. M. Quiney, C. Q. Tran, and K. A. Nugent, Opt. Lett. **34**, 2198 (2009).
[24] L. W. Whitehead, G. J. Williams, H. M. Quiney, D. J. Vine, R. A. Dilanian, S. Flewett, K. A. Nugent, A. G. Peele, E. Balaur, and I. McNulty, Phys. Rev. Lett. **103**, 243902 (2009).
[25] J. Clark, X. Huang, R. Harder, and I. Robinson, Nat. Commun. **3**, 993 (2012).
[26] X. Huang, R. Harder, S. Leake, J. Clark, and I. Robinson, J. Appl. Crystallogr. **45**, 778 (2012).
[27] J. N. Clark and A. G. Peele, Appl. Phys. Lett. **99**, 154103 (2011).
[28] An incoherent description of the source is possible due to the relatively large source size [29] used on ID01.
[29] I. A. Vartanyants and A. Singer, New J. Phys. **12**, 035004 (2010).
[30] O. Moutanabbir, M. Reiche, N. Zakharov, F. Naumann, and M. Petzold, Nanotechnology **22**, 045701 (2011).
[31] V. Favre-Nicolin, J. Coraux, M.-I. Richard, and H. Renevier, J. Appl. Crystallogr. **44**, 635 (2011).
[32] V. Favre-Nicolin, F. Mastropietro, J. Eymery, D. Camacho, Y. M. Niquet, B. M. Borg, M. E. Messing, L.-E. Wernersson, R. E. Algra, E. P. A. M. Bakkers *et al.*, New J. Phys. **12**, 035013 (2010).
[33] M. Falcioni and M. W. Deem, J. Chem. Phys. **110**, 1754 (1999).
[34] S. Marchesini *et al.*, Opt. Express **11**, 2344 (2003).
[35] S. M. Polvino, C. E. Murray, Ö. Kalenci, I. C. Noyan, B. Lai, and Z. Cai, Appl. Phys. Lett. **92**, 224105 (2008).
[36] V. Favre-Nicolin, J. Eymery, R. Koester, and P. Gentile, Phys. Rev. B **79**, 195401 (2009).
[37] X. Shi, G. Xiong, X. Huang, R. Harder, and I. Robinson, New J. Phys. **14**, 063029 (2012).
[38] C. Claeys, E. Simoen, S. Put, G. Giusi, and F. Crupi, Solid State Electron. **52**, 1115 (2008).
[39] N. Hrauda *et al.*, Nano Lett. **11**, 2875 (2011).